Vol. 08, No. 2 (2026) 1133-1142, doi: 10.24874/PES08.02B.004

Proceedings on Engineering Sciences

www.pesjournal.net

TECHNOLOGY FOR PRODUCING PIEZOELECTRIC PICOLITER DISPENSERS FOR DIRECT BONDING DNA PRINTING SYSTEMS

Timofey Akulinin[1]
Denis Nepomnyashchikh
Alena Talovskaya
Evgeny Barbin
Ivan Kulinich

Received 28.01.2026.
Revised 18.05.2026.
Accepted 09.06.2026.

Keywords:

DNA printing, Liquid microdispenser, Silicon substrate, Direct bonding, Surface activation, Roughness, Bond strength, Picoliter

A B S T R A C T

The article presents a technology for producing a picoliter-range liquid microdispenser based on silicon substrates using the method of direct silicon-to-silicon bonding. The chemical cleaning and activation modes of surfaces and bonding parameters are described. The influence of roughness on the bonding results is investigated, and tests are conducted on the rupture strength of 10 samples and droplet formation.

© 2026 Published by Faculty of Engineering

1. INTRODUCTION

In recent years, synthetic DNA has become an indispensable tool in modern science and technology, being used in research in molecular biology, nanotechnology, bioinformatics, and data storage systems (Yu et al., 2024). To implement such projects, it is necessary to create DNA with a given sequence in laboratory conditions, with particular importance being attached to methods that ensure high accuracy, reproducibility, and automation of the process (Hughes & Ellington, 2017). One promising area is DNA printing technology, based on the principles of additive synthesis, in which nucleotides are sequentially added to a substrate or reaction zone using controlled microdispensers (Kim et al., 2024). Unlike traditional phosphoramidite synthesis, DNA printing reduces reagent volumes and increases the scalability and flexibility of processes. At the same time, this technology faces a number of fundamental problems related to the limited functional stability of printed DNA chains, whose active life in the reaction environment does not exceed several days (Deng et al., 2024). This imposes restrictions on the length of synthesized sequences and requires an increase in printing speed to minimize the destruction of active sites and the degradation of intermediate structures. An additional limiting factor in Russia in the field of synthetic DNA research is the lack of commercial offerings and technological solutions for forming DNA chains based

[1] Corresponding author: Timofey Akulinin
Email: akulinin.tima@gmail.com

on domestically produced DNA printers. Accordingly, research into the development of DNA printers and their components is a pressing task. Of particular interest is the development of micro-dispensers capable of stable single-droplet generation in the picoliter range at high operating frequencies. Further advancement of DNA printing as a technological platform requires not only improvements in chemical synthesis protocols but also enhanced precision in reagent delivery, which is directly determined by the performance of microfluidic and piezoelectric elements within the dispensing system.

The use of silicon substrates and microelectronic fabrication technologies enables the formation of highly reproducible microchannel and membrane geometries, providing controlled acoustic regimes for droplet generation. In this context, the choice of microstructure sealing and bonding methods becomes critically important, as it defines the mechanical integrity, chemical purity, and long-term stability of the dispenser during operation with biological solutions. Direct silicon bonding is therefore considered one of the most promising approaches, allowing the formation of monolithic structures without intermediate layers that could adversely affect the dispensing process.

The core element of such systems is a microdispenser that ensures the formation and precise dosing of microdroplets of oligonucleotide solution. The stability, reproducibility, and volume range of dosing directly affect the accuracy of DNA chain assembly and the quality of the resulting biomaterial.

Existing dosing methods used in microdosing systems include thermal jet, electrostatic, and piezoelectric principles of operation. However, thermal jet dispensers, which use local heating of the liquid, are unsuitable for working with biomolecule solutions, as high temperatures lead to DNA denaturation and nucleotide degradation. Electrostatic methods, based on accelerating droplets in an electric field, are limited in frequency range, require high voltages, and do not provide stable droplet ejection at low volumes. Thus, the only technically sound solution remains a piezoelectric microdispenser, which ensures precise droplet formation by generating acoustic waves during mechanical deformation of the piezoelectric element (Kim et al., 2024; Deng et al., 2024).

Piezoelectric microdispensers operating in a drop-on-demand mode generate microdroplets of a specified volume without contact with the target surface. When an electrical pulse is applied, the piezoelectric actuator bends a diaphragm, compressing the liquid in the chamber and ejecting a droplet through the nozzle (Nanolitre Dosage). After the pulse, the diaphragm returns to its initial position, and the dispenser is self-refilled. Such systems typically operate with low-viscosity liquids (up to approximately 5 mPa·s at room temperature). Typical droplet volumes range from tens of picoliters to units of nanoliters. For example, the standard GeSiM SPIP dispenser produces droplets of 0.6–1.1 nL, while the GeSiM PicPIP produces droplets of 0.1–0.2 nL. The actuation frequency can reach several hundred to thousands of hertz (up to 500–1000 Hz, depending on viscosity) (Nanolitre Dosage).

Several leading manufacturers of such systems are represented on the market. Among German companies, GeSiM (Nano-Plotter series) is a key supplier of MEMS dispensers for biomedical applications, providing droplet volumes of 0.05–1.1 nL and supporting aqueous solutions, buffers, and redox reagent solutions; highly viscous adhesives are handled by separate systems (Nano-PlotterTM, GESIM, n.d.). Another major German manufacturer is VERMES Microdispensing. VERMES produces dispensers for medium and very high viscosities; for example, the MDS 3200+ series is designed for liquids with viscosities up to 2·10^6 mPa·s (pastes, silicones, highly filled adhesives), operates continuously at frequencies up to 1000 Hz, and generates droplets with diameters below 150 µm (Microdispensing System - MDS 3200+, VERMES Microdispensing, n.d.). Microdrop Technologies (Germany) offers piezoelectric dispensers based on inkjet technology, producing droplets of 20–380 pL (0.02–0.38 nL) with a repeatability of approximately 1% and operating frequencies up to 2000 Hz.

In China, several companies have emerged offering analogues of European dispensers. Wowei (Shenzhen) manufactures systems analogous to the MDS 3200+; according to the manufacturer's specifications, their operating viscosity range is approximately 1–100 000 cP (mPa·s), making them suitable for dispensing adhesives and resins (Micro Dispensing System - Mds 3200+, Maikeduo, n.d.). China is also actively developing liquid printing systems based on piezoelectric nozzles, which are used in particular for 3D bioprinting and microfluidic chip fabrication.

In the United States, BioDot offers the BioJet system, a dispensing module combining a piezoelectric valve with a high-precision syringe drive. This system dispenses droplets in the range of 2–2000 nL and is intended for analytical applications, PCR, and related biomedical assays (Technologies BioJetTM, Biodot, n.d.).

There are only a few types of dispensers used for DNA printing on the market. Microdispensers must meet requirements for high precision in droplet formation in the picoliter and nanoliter range, stability of dispensing volume, and repeatability of discharge at frequencies up to tens of kilohertz. The design of the dispenser must ensure that there is no thermal or electrostatic impact on the biomaterial, that the surfaces are chemically inert, and that it is compatible with DNA solutions (Deng et al., 2024). The characteristics of microdispensers used in DNA printing are presented in Table 1.

Table 1. Characteristics of microdispensers.

Manufacturer / Model	Dose volume	Viscosity range	Frequency (Hz)	Liquids (examples)
GeSiM (Germany) (Nano-PlotterTM) – SPIP/PicPIP	0.6–1.1 nl (SPIP); 0.1–0.2 nl (PicPIP)	up to ~5 mPa·s (at T ≈ 20°C)	up to ~500–1000	Biological solutions (buffers, DMSO), organic
Scienion sciFLEXARRAYER S3 (Germany) (Fox et al., 2017)	30–800 pcl	≈1–10 mPa·s (buffers, DNA/protein samples)	-	Biomaterials (DNA, proteins), PCR solutions
VERMES MDS 3200+ (Germany)	droplet diameter <150 µm	supported viscosity up to 2×10^6 mPa·s	operating frequency up to 1000 Hz	ntended for dispensing silicones, pastes, and highly viscous adhesives
VERMES MDS 3280 (Germany)	droplet diameter <150 µm	supported viscosity up to 2×10^6 mPa·s when heating is applied	operating frequency up to 1000 Hz	designed for very high-viscosity adhesives and substrate materials, including high-temperature variants
Microdrop MD series (Germany)	droplet volumes of 20–380 pL (depending on nozzle diameter)	supported viscosity range 0.4–20 mPa·s without heating, up to 100 mPa·s with tip heating, and up to 10^4 mPa·s with full heating	operating frequency from 1 to 2000 Hz	suitable for free polymers, waxes, low-viscosity adhesives, and chemically aggressive media due to the use of glass and PTFE wetted components
BioDot BioJet (US) (Technologies BioJetTM)	2–2000 nl	(water-soluble media)	-	Analytical reagents, PCR materials
Wowei (China) – MDS 3200+ analogue	droplet diameter <150 µm	viscosity range 1–100 000 cP (1–100 000 mPa·s)	operating frequency up to 1000 Hz	intended for dispensing viscous adhesives and resins

A comparison of dispensers shows that GeSiM and Scienion devices are best suited for DNA printing due to their small dispensing volumes (down to the picoliter range), high operating frequency, and compatibility with low-viscosity biological solutions. BioDot BioJet is designed for larger volumes (nanoliter range) and is therefore effective in analytical and diagnostic systems, but less applicable in high-precision DNA printing.
Such dispensers are manufactured using two-plate semiconductor technologies, in which microchannels are formed for fluid delivery. Various bonding technologies can be used to connect the plates and form sealed channels: direct, anodic (Suni, 2006), bonding with intermediate layers (polymers, metals, bonding adhesives, etc.).

Given the specifics and high requirements for the shape and cross-sectional area of the microchannel necessary for the accurate formation of droplets of the required volume, the use of connections with intermediate layers is extremely difficult. Uneven channel cross-sectional area and adhesive leakage into the channel may occur, which negatively affects the dosing parameters, therefore, either direct or anodic bonding is used for the manufacture of dispensers. Both allow the formation of monolithic microstructures without the use of adhesive materials. This technology ensures high chemical purity, mechanical strength, and tightness of connections, which is critically important when creating dispensers for working with biological solutions (Suni, 2006).

The scientific novelty of this study lies in the fact that, for the first time in Russia, a micro-dispenser for DNA printing has been manufactured. The article presents the technological stages of its manufacture, as well as experimental results confirming the formation of single liquid droplets. The results obtained demonstrate the possibility of using direct plate splicing technology to create domestic micro-dispensers designed for DNA printing systems and other areas of biomedical microelectronics.

2. MODELING OF YHE PROCESS IN COMSOL MULTIPHYSICS

COMSOL Multiphysics is an advanced software package for modeling and simulation of a wide range of physical phenomena. The software enables the creation of high-accuracy computational models, which is essential for the analysis of complex systems involving interactions between different physical processes. The platform is based on the finite element method (FEM), which provides accurate numerical solutions of differential equations describing physical processes.

One of the key capabilities of COMSOL Multiphysics is the simulation of laminar fluid flows. Laminar flow is a flow regime in which the fluid moves in parallel layers without mixing, which is important for many engineering and scientific applications, including hydrodynamic analysis, microfluidics, and chemical processes. Accurate modeling of such flows makes it possible to predict fluid behavior in systems, optimize their performance, and calculate the fluid dynamics within a dispenser.

Another essential feature for simulating droplet formation at a dispenser nozzle is the level set method, which is used to track and model moving interfaces between two media. This approach is particularly useful in problems where phase interactions must be taken into account, such as during the interaction of liquid and gas phases or the mixing of different liquids (Fontes, 2025).

Multiphysics modeling in COMSOL makes it possible to combine various physical phenomena within a single model while accounting for their mutual interactions. This significantly expands analytical capabilities and enables the study of complex systems in which thermal, mechanical, electrical, and other processes interact.

The following section describes a methodology for modeling the physical processes governing liquid behavior in dispensers using the Laminar Flow and Level Set interfaces.

The Level Set interface in COMSOL Multiphysics employs a reinitialized, conservative level set method to describe and transport the fluid interface. The reinitialized method involves periodic updating (reinitialization) of the level set function, which is used to represent the interface between phases (for example, liquid and gas). Reinitialization helps maintain stability and accuracy of the interface description over time, preventing the accumulation of numerical errors.

The conservative formulation of the level set method implies preservation of certain physical properties of the system, such as liquid volume, during interface transport and deformation. This is particularly important for accurate modeling of processes in which mass conservation is a critical requirement (Fontes, 2025).

The contour φ = 0.5 of the level set function defines the phase boundary, where φ = 0 corresponds to air and φ = 1 corresponds to liquid. Within the transition layer adjacent to the interface, the value of φ varies smoothly from 0 to 1. The interface is advected with the fluid velocity u at the boundary. The equation describing convection of the reinitialized level set function is given by

$$\frac{\partial \varphi}{\partial t} + u \cdot \nabla \phi = \gamma \left(\nabla \cdot \left(\frac{\nabla \varphi}{|\nabla \varphi|} \right) - \frac{\varphi - \varphi_0}{\varepsilon} \right), \qquad (2.1)$$

where φ is the level set function, u is the fluid velocity, γ is the reinitialization parameter, and ε is the thickness of the transition layer.

The level set function is also used to smooth discontinuities in density and viscosity across the interface according to the following definitions:

$$\begin{aligned} \rho &= \rho_{air} + (\rho_{ink} - \rho_{air})\varphi, \\ \mu &= \mu_{air} + (\mu_{ink} - \mu_{air})\varphi \end{aligned} \qquad (2.2)$$

where ρ and μ denote density and dynamic viscosity, respectively, and φ is the level set function varying from 0 to 1 within the transition layer.

The Navier–Stokes equations for an incompressible fluid, including surface tension effects, describe mass and momentum transport. Ink and air can be considered incompressible if the fluid velocity is small compared to the speed of sound. The Navier–Stokes equations take the following form:

$$\rho \left(\frac{\partial u}{\partial t} + u \cdot \nabla u \right) - \nabla \cdot \left(\mu \left(\nabla u + \nabla u^T \right) \right) + \nabla p = F_{st} \qquad (2.3)$$

where ∇p is the pressure gradient and F is the surface tension force.

The continuity equation for incompressible flow is expressed as

$$\nabla \cdot u = 0, \qquad (2.4)$$

This equation represents conservation of mass in the fluid flow. In the context of the Navier–Stokes equations, it ensures that the fluid preserves its volume in both time and space (Taratuta, 2020).

The surface tension force is defined as

$$F_{st} = \sigma \delta \kappa n, \qquad (2.5)$$

where n is the normal vector to the interface, σ is the surface tension coefficient (N/m), κ is the curvature, and δ is the Dirac delta function, which is nonzero only at the fluid interface.

The interface normal vector is given by

$$n = \frac{\nabla \varphi}{|\nabla \varphi|}, \qquad (2.6)$$

An approximation of the Dirac delta function is defined as

$$\delta = 6|\,\phi(1-\phi)|\;|\,\nabla \phi|\,, \qquad (2.7)$$

Boundary conditions.

At the nozzle inlet, a function describing the inlet flow velocity in the z-direction is applied. The velocity increases from 0 to 8 μL/s during the first 2 μs, is maintained at this level for 10 μs, and then decreases back to 0 over the next 2 μs. Thus, the time-dependent average velocity in the z-direction can be defined as

$$u_{av}(t) = rect(t) \cdot 8 \cdot 10^{-6}, \qquad (2.8)$$

where t is given in seconds and rect(t) is a rectangular pulse function with transition points at 1 μs and 10 μs and a transition duration of 2 μs.

At the nozzle outlet, a constant pressure condition is imposed. In this case, the absolute pressure value is not significant, since the velocity field depends only on the pressure gradient; therefore, the resulting velocity field at the outlet remains unchanged.

On all other boundaries, a no-slip boundary condition is applied.
To model the droplet behavior, a 2D model was developed. The geometry of the model is shown in Figure 1.

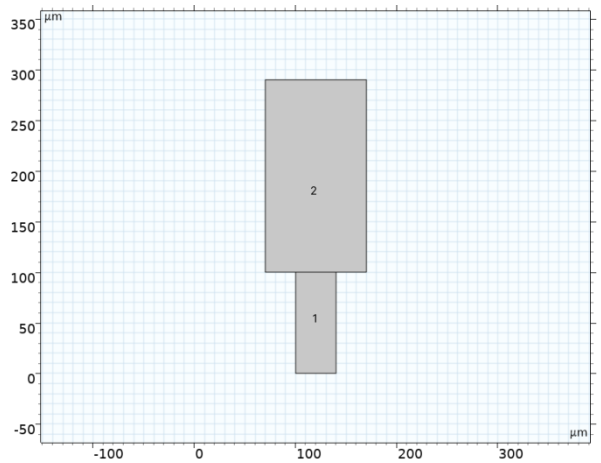


Figure 1. Screenshot of the 2D model geometry: 1 – nozzle; 2 – air domain

The nozzle length is 40 μm; the air domain is required to simulate the droplet flight in space. Using the Laminar Flow and Level Set physics interfaces, the result shown in Figure 2 was obtained. The boundary conditions applied to the model were defined in accordance with Equation (2.8).

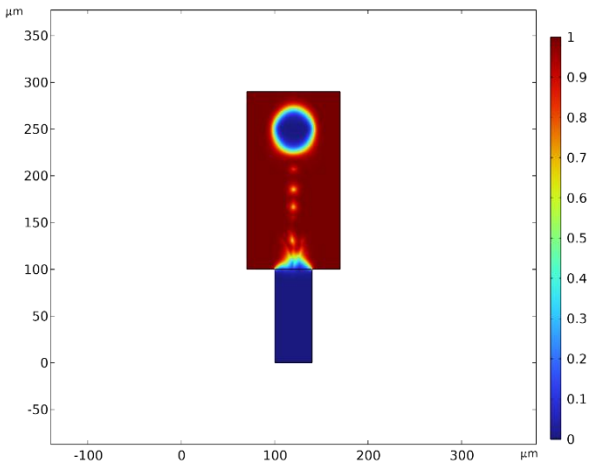


Figure 2. Screenshot of the droplet simulation result at a time of 70 μs

Thus, the 2D simulation demonstrates that, for the specified velocity parameters, excitation pulse, and geometric dimensions, stable droplet formation occurs. The next stage of the study involves the development of a 3D model based on the results obtained from the 2D simulation. The channel width in the nozzle region is 50 μm. Figure 3 shows the geometry of the 3D structure used for simulating droplet behavior.

The performed numerical modeling demonstrates that, at the specified excitation pulse parameters obtained experimentally, stable droplet formation is achieved. Both the 2D and 3D simulations confirm the emergence, necking, and subsequent detachment of a single liquid droplet at the nozzle exit, indicating that the selected pulse amplitude and duration are sufficient to overcome surface tension forces and ensure controlled ejection of the liquid.

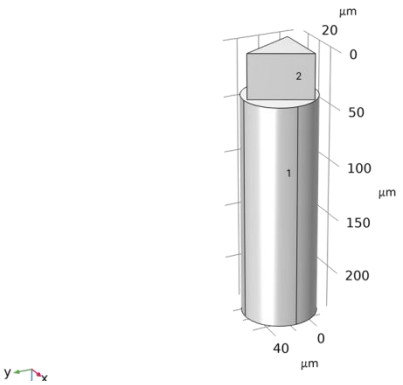


Figure 3. Screenshot of the 3D geometry used for simulation: 1 – air domain; 2 – nozzle

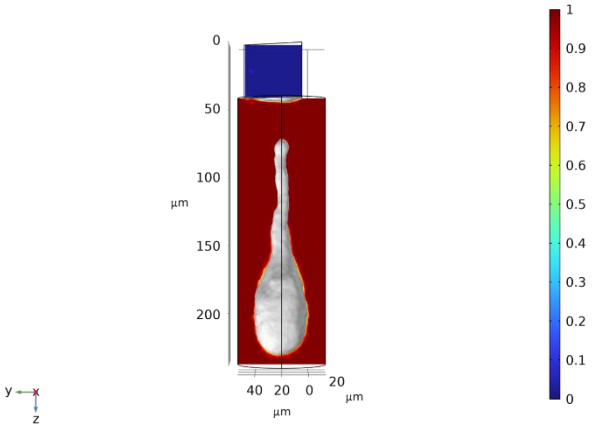


Figure 4. Screenshot of the droplet simulation result at a time of 30 μs

3. TECHNOLOGICAL PROCESS FOR PRODUCTION OF DISPENSERS

The design of the microdispenser developed (Kulinich et al., 2023) is shown in Figure 1 and provides for its attachment by the housing 1 to the working unit of the DNA printing printer. The oligonucleotide solution is supplied from the DNA printer reservoir through a polymer tube connected to pipe 2. The dispenser body 3 is fixed in sleeve 4, which is screwed into housing 1. After the microchannel is filled with solution, an electrical signal of the required shape, frequency, and voltage is applied to the piezoelectric element 5. As a result, the piezoelectric element excites the membrane vibrations, which leads to the generation of an acoustic wave in the liquid channel. Under the action of this

wave, a drop is ejected through the nozzle of the dispenser 6.

A technological process was developed for the manufacture of dispensers, as shown in Figure 6. Two silicon wafers 100KEF-(3.6-5.4) (100)-385+/-5, DP, BPKZh.90.01.000.TU were used as blanks. One of them is used to form microchannels and windows for the piezoelectric element, the second is used to seal the channel and is used at the bonding stage. Both plates were pre-cleaned in dimethylformamide (DMF) to remove organic and inorganic contaminants. The operation was carried out at a temperature of 80°C for 5 minutes, followed by rinsing in deionized water and drying under a stream of nitrogen.

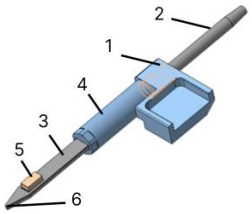


Figure 5. Schematic diagram of the dispenser: 1 – housing; 2 – pipe; 3 – dispenser body; 4 – sleeve; 5 – piezoelectric element; 6 – nozzle.

The first stage (Figure 6a) involves thermal annealing of silicon on the first plate to form a dielectric mask from silicon oxide, which is carried out in a muffle furnace at a temperature of 1000 °C for 12 hours.

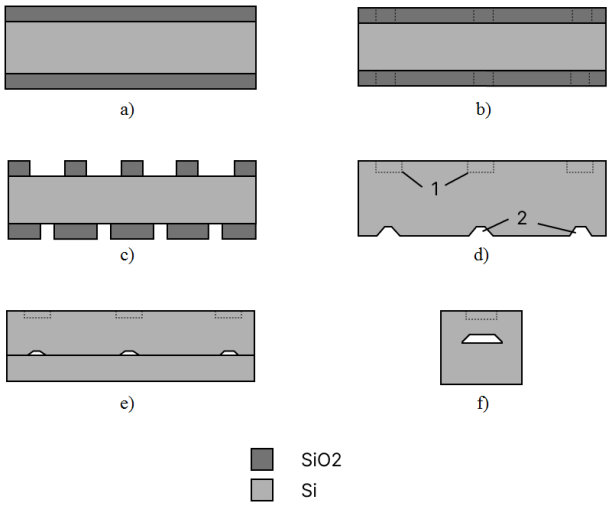


Figure 6. Schematic diagram of the dispenser producing process: 1 – windows for the piezoelectric element; 2 – microchannel

After oxidation, the second stage is the formation of alignment marks in the dielectric mask on both sides of the plate (Figure 6b). At this stage, AZ1505 photoresist was used, which was applied on both sides by centrifugation at a speed of 1000 rpm and an acceleration of 400 rpm. The photoresist was exposed using contact photolithography on a photomask. The final step at this stage was to remove the photoresist (AZ developer).

The third stage involved opening windows in the dielectric mask for subsequent silicon etching (Figure 6c). The photoresist was formed in the same way as in the second stage. Exposure was carried out using laser photolithography on the upper and lower sides of the working plate according to the formed alignment marks. The fourth stage is the formation of microchannels 2 and windows 1 for piezoelectric elements (Figure 6d). Silicon etching was performed on a previously formed silicon oxide dielectric mask (Figure 6c) in a 10% TMAN solution with the addition of ammonium persulfate $(NH_4)_2S_2O_8$ 5% for 2 hours at 75°C. Silicon oxide removal was performed in a buffer etchant.

In the fifth stage, both plates are separated by disc cutting into samples measuring 20x30 mm, where 5 microchannels are placed, after which they undergo a bonding process, a detailed description of which is given in section 3 (Figure 6e).

The final stage is disc cutting of the samples into individual dispenser bodies (Figure 6e) and assembly of the dispenser (Figure 5) (Akulinin et al., 2022).

4. STUDY OF THE EFFECT OF ROUGHNESS ON BONDING STRENGTH

In direct bonding of silicon wafers, the formation of interatomic bonds occurs at a limited number of actual contact points determined by the surface microrelief. An increase in surface roughness reduces the real contact area between the surfaces and increases the probability of enclosed void formation at the bonding interface, which directly affects the strength of the resulting bond. Therefore, quantitative evaluation of silicon surface roughness is a necessary step in the analysis of conditions required to obtain a mechanically strong inter-wafer bond.

To study the effect of roughness on bonding strength, five silicon samples with formed microchannels with a joint surface area of 34.26 mm2 and different roughness were taken. Numerical roughness values for all samples were obtained using a PROFILM 3D optical profilometer. An example of a sample scan is shown in Figure 7.

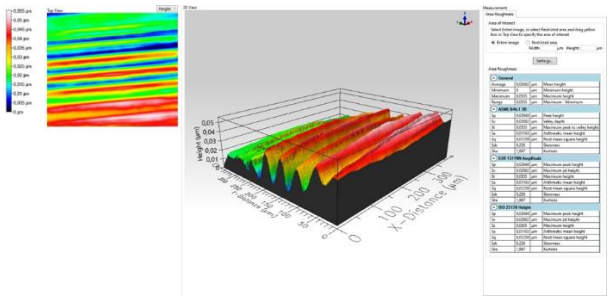


Figure 7. Screenshot of the scan result for the surface of a silicon wafer sample

The scan data obtained for the surfaces of all five silicon wafers are shown in Table 2.

Table 2. Surface roughness Ra.

Sample	Surface roughness, μm
1	0.01103
2	0.01064
3	0.007526
4	0.006142
5	0.7079

Before the bonding operation, the samples underwent comprehensive preparation, including initial and chemical treatment stages.

During the initial treatment stage, the samples were pre-cleaned in a dimethylformamide (DMF) solution at a temperature of 80 °C for 5 minutes. This was followed by mechanical grinding of the surfaces in the same solution to remove surface contaminants and any remaining process materials. Next, ultrasonic treatment in DMF was performed for 2 minutes to further remove microparticles and organic contaminants. After this procedure, the samples were rinsed in deionized (DI) water, cleaned in isopropyl alcohol (IPA) at a temperature of 80 °C for 5 minutes, and then subjected to ultrasonic cleaning in IPA for 2 minutes. This stage was completed by re-washing the samples in DI water.

Chemical treatment included two-stage surface etching. In the first stage, an SPM solution was used, which is a mixture of sulfuric acid, hydrogen peroxide, and water in a ratio of 1:1:5. Treatment in this solution was carried out with an exposure time of 20 minutes. In the second stage, an RCA solution consisting of ammonia, hydrogen peroxide, and water in a ratio of 1:1:5 was used, also with a treatment time of 20 minutes. After completion of chemical etching, the samples were rinsed in DI water and dried under controlled conditions.

To increase surface activity and improve the quality of interfacial contact, activation was carried out in oxygen plasma at a power of 300 W and a processing time of 1.5 minutes. After plasma activation, the samples were additionally rinsed in DI water in an ultrasonic bath for 2 minutes and dried.

The final stage of preparation was the connection of the treated samples and the bonding process on a manual bonding fixture, which consists of two clamping plates fixed together with a bolt connection (see Figure 8).

Bolts 1 are screwed into metal clamping plates 2, the surface of which has been polished and hardened. Samples 3 to be bonded are placed between the clamping plates 2. The bolts are tightened in the order shown in Figure 5.

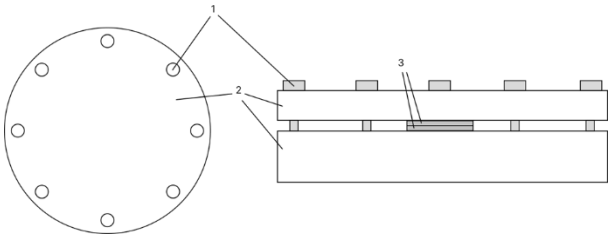


Figure 8. Schematic view of manual equipment for the direct bonding process: 1 – bolts; 2 – clamping plates; 3 – silicon wafers

During the direct bonding process of silicon wafers, an applied pressure of approximately 50 MPa was used to ensure a reliable interatomic connection on the contact surface (Li et al., 2020).

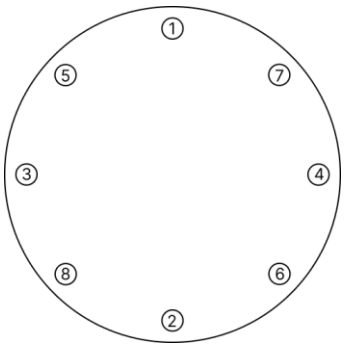


Figure 9. Bolt tightening sequence diagram

To estimate the required pressing force *F*, the following equation was used

$$F = P \cdot S \,, \tag{1}$$

where *P* is the applied pressure; *S* is the active contact surface area.

According to equation (1)

$$F = 5 \cdot 10^7 \cdot 0.0003 = 15000\ H$$

Formula for calculating the tightening torque of one small bolt

$$M = k \frac{d_T}{z} F \,, \tag{2}$$

where *z* is the number of bolts, 8; d_T is the bolt thread diameter, 0.006 mm; *k* is the friction coefficient, 0.2.

Calculation of the tightening torque for one bolt using formula 2:

$$M = 0,2 \cdot \frac{0,006}{8} \cdot 15000 = 2,27\ N \cdot m \,.$$

Thus, to obtain the maximum pressure inside the system on the silicon, each bolt must be tightened with a torque of 2.27 N·m.

The bolts were tightened in 90° increments until they were in firm contact, then the bolts were tightened in 0.2 N·m increments. The force was controlled by a torque wrench. Thickness gauges were used between the clamping plates to control the uniformity of the pressure.

As a result of the experiments, samples No. 2, 3, and 4 were bonded, which is explained by their lower surface roughness compared to other samples. Minimal roughness provides a smoother surface, which promotes tighter contact between surfaces, resulting in a more reliable connection.

For the tensile test, 10 silicon dispensers were produced from plates with a surface roughness of no more than 6 nm.

The dispenser samples were subjected to tensile testing on the dynamometer shown in Figure 10 in order to evaluate the strength of the direct bonding connection.



Figure 10. MEGEON 03500 dynamometer

The interaction between the dispenser and the dynamometer is shown in Figure 11.

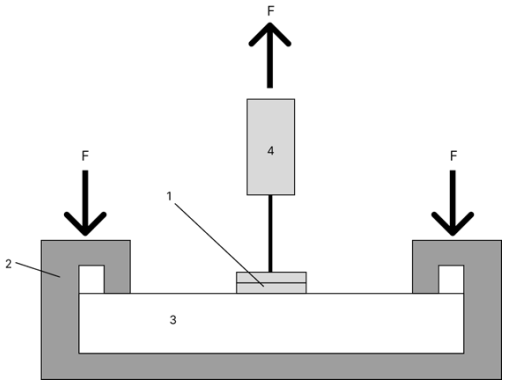


Figure 11. Schematic diagram: 1 – dispenser; 2 – dynamometer table; 3 – pedestal; 4 – dynamometer

Dispenser 1 is glued to pedestal 3, which is secured to table 2 with clamps, and then attached to dynamometer 4 with a wire connection using lead-tin solder.

The minimum tear-off force was 6.4 N, the maximum was 11.8 N, and the average force was 9.47 N. On all samples, the tear-off occurred along the structure of the upper silicon plate above the bonding boundary, which indicates that the bonding strength is higher than the strength limit of silicon.

Table 3. Experimental data.

No.	*F*, N
1	6.4
2	11.8
3	10.4
4	9.2
5	7.7
6	9.4
7	10.8
8	8.3
9	7.2
10	9.5

Samples were obtained that were tested by droplet formation. Figure 12 shows a stroboscopic camera image of the droplet ejection process.

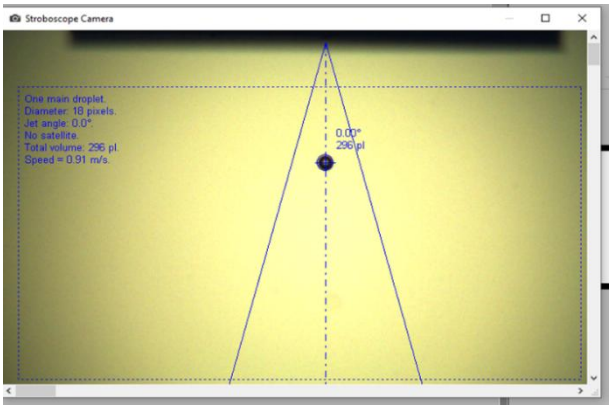


Figure 12. Stroboscopic photography of the dosing process

It can be seen that when a pulse with duration of 80 μs, amplitude of 80 V, and frequency of 100 Hz is applied to the piezoelectric element, a single droplet with a volume of 296 pL is formed. The ejection velocity was approximately 0.9 m/s, with no satellite droplets observed, indicating the stability of the acoustic dosing mode. The study of the dependencies of the characteristics of the obtained dispensers is the subject of further research.

5. CONCLUSION

A technology has been developed for producing a liquid micro-dispenser based on a silicon substrate using the direct bonding method, which includes the formation of microchannels by liquid etching in a TMAN solution, surface activation, alignment, and annealing.

It has been shown that for successful direct bonding, preliminary chemical and plasma activation of the

surface is necessary, as well as compliance with roughness requirements: it must be less than 10 nm. It has been established that as roughness increases, the strength of the bond decreases.

A technological process for producing the dispenser has been developed, including the following sequential stages: thermal oxidation, photolithography, etching, cutting, bonding, and final assembly of the device.

During tensile tests on a dynamometer, all samples tested failed in the area where the dispenser was attached to the device clamps, while the joint area obtained by direct bonding remained intact. The absence of traces of destruction along the bonding boundary indicates that the strength of the formed connection exceeds the strength limit of silicon. This result confirms the high quality of interfacial adhesion and the correctness of the selected bonding process mode. The droplet volume of the produced dispenser was 296 pL, which meets the requirements for print heads for DNA printers. The obtained results demonstrate the high potential of direct silicon bonding technology for the fabrication of high-precision piezoelectric micro-dispensers operating in the picoliter range. The proposed technological route can be further applied to optimize microchannel geometry, increase operating frequencies, and integrate dispensers into functional DNA printing modules.

The experimental results confirm that the surface preparation parameters of silicon wafers, particularly surface roughness, are a determining factor in the formation of a strong inter-wafer bond using the direct bonding method. The established relationship between roughness values and bonding success allows this parameter to be considered critical in the development of fabrication routes for silicon-based micro-dispensers.

It is shown that the use of direct bonding enables the formation of hermetic and mechanically robust joints that maintain integrity during tensile testing and ensure stable dispenser operation in single-droplet generation modes. The obtained results provide a foundation for further optimization of geometrical and technological parameters of micro-dispensers, as well as for extending their operational performance in high-precision micro-dispensing applications.

Acknowledgements: The research results were obtained with the support of the Ministry of Science and Higher Education of the Russian Federation (theme no. FEWM-2024-0008).

References:

Akulinin, T. A., Kulinich, I. V., Kazimirov, A. I., & Troyan, P. E. (2022). Liquid piezoelectric microdispenser based on a silicon substrate. XVIII International Scientific-practical Conference “Electronic Devices and Control Systems”, Tomsk, Russia, 16–18 November 2022, pp. 66–69.

Deng, X., Li, H., & Song, Y. (2024). Inkjet printing-based high-throughput DNA synthesis. *Giant*, *17*, 100222. doi: 10.1016/j.giant.2023.100222.

Fox, C. B., Nemeth, C. L., Chevalier, R. W., Cantlon, J., Bogdanoff, D. B., Hsiao, J. C., & Desai, T. A. (2017). Picoliter-volume inkjet printing into planar microdevice reservoirs for low-waste, high-capacity drug loading. *Bioengineering & Translational Medicine*, *2*(1), 9–16. doi: 10.1002/btm2.10053.

Fontes, E. (2025). *Two Methods for Modeling Free Surfaces in COMSOL Multiphysics®* Retrieved from https://www.comsol.com/blogs/two-methods-for-modeling-free-surfaces-in-comsol-multiphysic

Hughes, R. A., & Ellington, A. D. (2017). Synthetic DNA Synthesis and Assembly: Putting the Synthetic in Synthetic Biology. *Cold Spring Harbor Perspectives in Biology*, *9*(1), a023812. doi: 10.1101/cshperspect.a023812.

Kim, J., Kim, H., & Bang, D. (2024). An open-source, 3D printed inkjet DNA synthesizer. *Scientific Reports*, *14*(1). doi: 10.1038/s41598-024-53944-x.

Kulinich, I. V., Gadirov, R. M., Loshchilov, A. G., & Borisov, A. V. (2023). Piezoelectric dispenser. Patent of the Russian Federation No. 2023131929, applied 05.12.2023, applicant: Tomsk State University of Control Systems and Radioelectronics , published 16.04.2024

Li, J., Jiang, Y., Li, H., Liang, X., Huang, M., Liu, D., & Zhang, D. (2020). Direct bonding of silicon carbide with hydrofluoric acid treatment for high-temperature pressure sensors. *Ceramics International*, *46*(3), 3944–3948. doi: 10.1016/j.ceramint.2019.10.123

VERMES Microdispensing (n.d.). *Microdispensing system - MDS 3200+*. Retrieved from https://www.vermes.com/products/piezo-based-systems/piezo-mds-3200

Maikeduo (n.d.) *Micro Dispensing System - Mds 3200+*. Retrieved from https://maikeduo.en.made-in-china.com/product/POHtsxzdhWGU/China-Micro-Dispensing-System-Mds-3200-.html#:~:text=Viscosity Range

GESIM (n.d.) *Nano-PlotterTM: The Versatile Non-Contact Microarray Printers*. Retrieved from https://gesim-bioinstruments-microfluidics.com/microarray-printer

GESIM (n.d.) *Nanolitre Dosage – Piezoelectric Dispensers Easy to Integrate*. Retrieved from https://gesim-bioinstruments-microfluidics.com/nanolitre-dosage/#:~:text=GeSiM

Suni, T. (2006). *Direct wafer bonding for MEMS and microelectronics.* VTT Technical Research Centre of Finland.

Taratuta, A. G. (2020). Navier–Stokes equations and their application in modeling. Scientific Community of Students of the 21st Century. Natural Sciences, p. 21.

Biodot (n.d.) *Technologies BioJetTM.* Retrieved from https://www.biodot.com/technology/biojet

Yu, M., Tang, X., Li, Z., Wang, W., Wang, S., Li, M., ... & Chen, C. (2024). High-throughput DNA synthesis for data storage. *Chemical Society Reviews*, *53*(9), 4463-4489. doi: 10.1039/d3cs00469d

Timofey Akulinin
Tomsk State University of Control Systems and Radioelectronics,
Tomsk,
Russia
akulinin.tima@gmail.com

Denis Nepomnyashchikh
Tomsk State University of Control Systems and Radioelectronics,
Tomsk,
Russia
nep_d@mail.ru

Alena Talovskaya
Tomsk State University of Control Systems and Radioelectronics,
Tomsk,
Russia
alena.a.talovskaia@tusur.ru
ORCID 0009-0001-6796-1135

Evgeny Barbin
Tomsk State University of Control Systems and Radioelectronics,
Tomsk,
Russia
evgenii.s.barbin@tusur.ru
ORCID 0000-0001-5904-0216

Ivan Kulinich
Tomsk State University of Control Systems and Radioelectronics,
Tomsk,
Russia
kulinich@tusur.ru
ORCID 0009-0001-0768-3495